

Higher-order topological insulators and superconductors protected by inversion symmetry

Eslam Khalaf^{1,2}

¹Max Planck Institute for Solid State Research, Heisenbergstr. 1, 70569 Stuttgart, Germany

²Department of Physics, Harvard University, Cambridge MA 02138

(Dated: December 14, 2024)

We study surface states of topological crystalline insulators and superconductors protected by inversion symmetry. These fall into the category of “higher-order” topological insulators and superconductors which possess surface states that propagate along one-dimensional curves (hinges) or are localized at some points (corners) on the surface. We show that the surface states of higher-order topological insulators and superconductors can be thought of as globally irremovable topological defects and provide a complete classification of these inversion-protected phases in any spatial dimension for the ten symmetry classes by means of a layer construction. Furthermore, we discuss possible physical realizations of such states starting with a time-reversal invariant topological insulator (class AII) in three dimensions or a time-reversal invariant topological superconductor (class DIII) in two or three dimensions. The former can be used to build a three-dimensional second-order topological insulator which exhibits one-dimensional chiral or helical modes propagating along opposite edges, whereas the latter enables the construction of three-dimensional third-order or two-dimensional second-order topological superconductors hosting Majorana zero modes localized to two opposite corners. Being protected by inversion, such states are not pinned to a specific pair of edges or corners thus offering the possibility of controlling their location by applying inversion-symmetric perturbations such as magnetic field.

I. INTRODUCTION

A topological insulator (TI) or superconductor (TSC) is characterized by a gapped bulk spectrum with gapless states on any given surface¹⁻⁴. The stability of these gapless surface states in a TI/TSC usually relies on the presence of local symmetries which include time-reversal symmetry (TRS) \mathcal{T} , particle-hole symmetry (PHS) \mathcal{P} , and their combination \mathcal{S} (usually called chiral symmetry). According to the presence or absence of these symmetries, gapped Hamiltonians have been classified into ten different symmetry classes by Altland and Zirnbauer (AZ)⁵. In any given dimension, five of these ten classes correspond to a TI/TSC⁶⁻⁸.

The concept of a TI/TSC can be extended to include gapped phases protected by crystalline symmetries which map different points in space to each other such as mirror, rotation, or inversion symmetries. These phases are called topological crystalline insulators (TCIs)^{9,10} and, unlike conventional TIs/TSCs, do not necessarily host gapless surface states on any given surface. Instead, surface states are only expected on surface planes which preserve the crystalline symmetry.

Recently, several works considered a class of TCIs which host surface states localized to the edges (hinges) or corners of a physical sample¹¹⁻¹⁶; these were dubbed higher-order TIs/TSCs^{11,12}. The surface of a k -th order TI/TSC in d dimensions is gapped except for a $(d - k)$ -dimensional region which hosts gapless modes. For example, a second-order TI in three dimensions hosts one-dimensional (1D) propagating modes localized to the sample hinges on an otherwise gapped two-dimensional (2D) surface. Notice that, in this terminology, a first-order TI/TSC is just a conventional (strong) TI/TSC. Examples of higher-order TIs/TSCs discussed in recent works include three-dimensional (3D) insulators with hinge modes protected by rotation¹⁴⁻¹⁶, mirror symmetry^{11,12,16,17}, or a combination of rotation and time-reversal¹¹ as well as 2D insulators with corner modes protected by mirror symmetry^{12,13,17}. Physical realizations of

higher-order TIs have recently been implemented in mechanical metamaterials¹⁸, electronic circuits¹⁹, and microwave resonators²⁰ and proposed to exist in several materials^{11,21,22}. In addition, some of the systems considered in earlier works where a magnetic field is applied to a 3D TI²³ or to ³He-B topological superfluid²⁴ also fall in the category of higher-order TIs/TSCs.

In this work, we show that higher-order TIs/TSCs can be protected by inversion symmetry alone and provide a complete classification of inversion-protected k -th order TIs/TSCs in any spatial dimension. The crucial difference between inversion symmetry and the spatial symmetries considered in earlier works^{11,12,14,17} lies in the fact that inversion does not leave any point on the surface invariant. This means that, in contrast to other symmetries such as rotation^{9,12} or mirror^{14,15}, inversion-protected surface states cannot be observed by considering some symmetry-invariant plane on the surface. Instead, they can only be captured on particular sample geometries by considering the surface as a whole. Furthermore, inversion-protected surface states are not expected to be pinned to a particular edge or corner, but instead can be localized at any pair of corners or edges related to each other by inversion. This particular property allows for the possibility of controlling their position by applying inversion-preserving perturbations such as magnetic field, as we will show later.

We will propose physical realizations for 3D second-order TIs, 3D second- and third-order TSCs and 2D second-order TSCs. The recipe for constructing these higher-order TIs/TSCs is to either apply a symmetry-breaking perturbation to a given strong (first-order) TI/TSC or to combine several strong TIs/TSCs such that the total strong index vanishes while preserving the symmetry. The latter approach was used to build higher-order TIs in class AII in Refs. 15 and 16, which constructed them by combining two time-reversal invariant 3D TIs in the presence of some spatial symmetries. The vanishing strong index implies that the surface can be gapped out by adding a mass term. The presence of spatial

symmetries may, however, cast some global constraints on this mass term, forcing it to vanish on some subregion on the surface, e.g. a line or a set of points, on which the Hamiltonian remains gapless. The resulting system implements a higher-order TI/TSC. For example, an inversion-protected second-order 3D TI with or without TRS can be respectively constructed by combining two 3D strong TIs or by applying a magnetic field to a 3D strong TI. In both cases, the resulting system is trivial from the point of view of the 3D topology due to the vanishing strong index, but implements a second-order TI hosting propagating 1D hinge modes due to inversion.

It should be noted that the dimensionality of surface states, and consequently the “order” of a certain TCI, cannot be generally defined without specifying the geometry and boundary conditions of the sample. For example, a 3D TCI protected by mirror symmetry exhibits 2D gapless surface states on any surface plane that is left invariant under mirror symmetry^{10,25}. On the other hand, placing the same TCI on a sphere (with open boundary conditions in all directions) yields 1D hinge modes propagating along the circle where the mirror plane intersects the sphere¹⁶. This issue arises whenever the spatial symmetry protecting the phase leaves some subregion (point, line, etc.) on the surface invariant, as noted in Ref. 16 which circumvented the difficulty by not referring explicitly to order and studying all TCIs that host anomalous surface states on some surface (dubbed “sTCIs”). For inversion symmetry, however, this issue is not relevant since its action does not leave any point on the surface invariant (assuming the inversion center is in the bulk of the sample). Hence, in this work we will refer explicitly to the order k of a higher-order TI/TSC to indicate the presence of $(d - k)$ -dimensional surface states on *any* compact inversion-symmetric surface.

We would like to stress that the higher-order TIs/TSCs considered in this work are proper bulk topological phases that can only be trivialized by going through a phase transition closing the *bulk* gap. This means that the surface states considered here are anomalous, i.e. they cannot exist in a stand-alone lower-dimensional system. Our definition of the phase is consistent with the definition given in Refs. 11 and 16, but differs from the definition used in Refs. 12 and 17, where phases related by a *surface* phase transition were considered topologically distinct.

We would also like to point out the relation between the phases considered here and the inversion-protected TCIs obtained using K-theory^{26,27}. The K-theory approach classifies phases as equivalence classes of bulk Hamiltonians that can be (stably) deformed into each other without closing the bulk gap or breaking the protecting symmetries. This means that the inversion-protected higher-order TIs/TSCs considered here are stable K-theory phases. On the other hand, it is easy to show that some of the K-theory phases do not possess any types of surface states and can thus be considered trivial from the perspective of surface states. Thus, the phases considered in this work form a proper subset of the inversion-protected phases obtained using K-theory in Refs. 26 and 27.

This paper is structured as follows. We start by summarizing the main argument used for understanding and classifying inversion-protected higher-order TIs/TSCs in Sec. II. We

show that the surface states of higher-order TIs/TSCs can generally be understood as “globally irremovable topological defects”. This is then used to derive a necessary condition for the existence of inversion-protected k -th order TI/TSC in any given dimension. In Sec. III, we propose physical realizations for 3D second-order TIs, 3D second- and third-order TSCs and 2D second-order TSCs. We discuss how these phases can be constructed by combining conventional TIs/TSCs or applying symmetry-breaking perturbations (e.g. magnetic field) to them and provide the pattern of surface states expected in each case. In Sec. IV, we make use of the layer construction introduced in Refs. 28 and 29 to provide a full classification of inversion-protected k -th order TI/TSC in any dimension leading to Table I. Afterwards, we provide a minimal Dirac model for the inversion-symmetric higher-order TIs/TSCs in any dimension in Sec. V. We close by making several concluding remarks regarding the stability of the phase against symmetry-breaking perturbations and the generalization to other spatial symmetries in Sec. VI.

II. SUMMARY OF THE ARGUMENT

We begin by summarizing our main argument for the construction and complete classification of inversion-protected higher-order TIs/TSCs. Following Ref. 16, we think of the surface states of higher-order TIs/TSCs as globally irremovable topological defects. Recall that a topological defect corresponds to a region in space, e.g. a domain wall, where some parameter in the Hamiltonian is changed such that it hosts zero energy states. Being topological means that the zero energy states are robust against any symmetry-preserving perturbations, but they can generally be moved freely. The simplest example of a topological defect is the surface of a strong TI/TSC which can be thought of as a domain wall between the bulk topological Hamiltonian and the trivial vacuum outside. More interesting examples include vortices in 2D $p_x + ip_y$ superconductors, which host Majorana zero modes^{30,31}, or dislocations in layered topological insulators³².

The local stability of a topological defect depends only on the dimension of the defect (which is the difference between the spatial dimension and the co-dimension of the defect) and the presence or absence of the local symmetries \mathcal{T} , \mathcal{P} , and \mathcal{S} ³². Using this knowledge, one can immediately deduce the classification of stable topological defects of a certain dimension from the classification of strong TIs/TSCs in one dimension higher. The resulting classification table in any dimension for the ten AZ classes was given in Ref. 32 and it is identical to the classification table of TIs/TSCs⁶⁻⁸ with the dimension shifted by 1. Similar to the classification of TIs/TSCs, topological defects of any given dimension are stable in five symmetry classes, three of which can host an arbitrary number of gapless states in the defect (\mathbb{Z} defects), while two can host at most one gapless state (\mathbb{Z}_2 defects).

In general, a topological defect on an otherwise gapped compact surface can always be removed³³. For instance, on the surface of a sphere, a line defect can always be deformed to a point. Similarly, point defects have to occur in pairs which

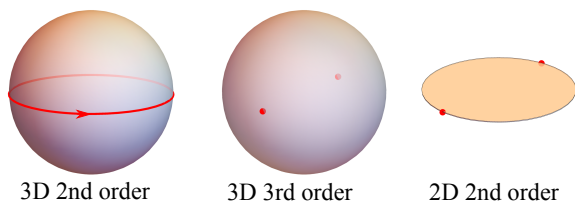


FIG. 1. Surface states of inversion-protected higher-order TI/TSC in two and three dimensions.

can be annihilated by bringing them together. Thus, despite their local stability, topological defects whose dimension is lower than that of the surface are globally unstable. Spatial symmetries, however, can make it impossible to remove these defects without breaking the symmetry. In the case of inversion, this follows from the fact that no point on the surface is left invariant by inversion, thus an inversion-symmetric topological defect can never be deformed to a point. For example, inversion forces a pair of point defects to be located at two inversion-related (antipodal points) which can never be brought together without breaking inversion. Likewise, a line defects will be confined to an inversion-symmetric curve that cannot be deformed to a point.

The correspondence between inversion-protected surface states and topological defects can be established by noting that inversion acts non-locally on the surface by mapping different points to each other, thus the only symmetries which can stabilize the gapless states locally are \mathcal{T} , \mathcal{P} , and \mathcal{S} . As a result, the surface states of an inversion-protected k -th order topological insulator in a given symmetry class in d dimensions are locally identical to $(d - k)$ -dimensional topological defects in the same class and are thus only stable if these defects are stable³⁴. Using the notation of Ref. 32, which labels the complex AZ classes by a \mathbb{Z}_2 variable $s_c = 0, 1$ for classes A and AIII, respectively, and the real AZ classes by a \mathbb{Z}_8 variable $s_r = 0, \dots, 7$ for classes AI, BDI, \dots , CI, respectively (cf. Table I), this conditions implies that an inversion-protected k -th order TI/TSC is possible in d dimensions when $s_c - d + k - 1 = 0 \pmod{2}$ for complex classes or when $s_r - d + k - 1 = 0, 1, 2, 4 \pmod{8}$ for real classes.

One specific feature of inversion-protected higher-order TIs/TSCs is that they always have a \mathbb{Z}_2 classification regardless of the underlying classification of the defects (this means that the stability of $(d - k)$ -dimensional topological defects is a necessary but not sufficient condition for the existence of an inversion-protected k -th order TI/TSC in d dimensions). The reason for this is that a pair of inversion-symmetric topological defects (notice that an inversion-symmetric 0D defect consists of two points) can each be deformed to a point without breaking inversion. This is achieved by ensuring they are related to each other by inversion at every stage of the process. This process is visually illustrated in Fig. 2 for zero- and one-dimensional defects on the surface of a sphere. The upper panel illustrates how two chiral modes living on a 1D curve on the surface, for example in class A, can be removed while preserving inversion. This process is equivalent to adding a

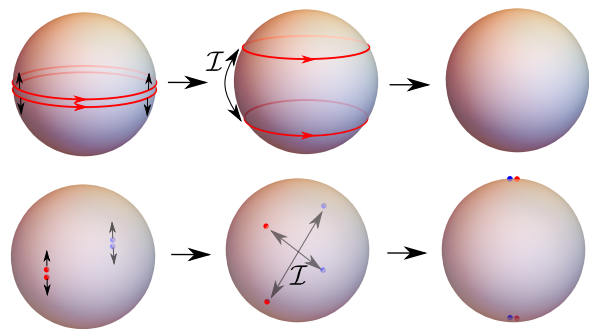


FIG. 2. The upper panel illustrates how two chiral modes can be removed without breaking inversion symmetry. The lower panel illustrates how a pair of 0D topological defects (each defect consists of two zero modes at two inversion related points with opposite chirality) can be removed by moving states of opposite chirality towards each other and annihilating them. As a result, the classification of inversion-protected higher-order TIs/TSCs is always \mathbb{Z}_2 regardless of the classification of the defect.

2D quantum Hall layer on the upper hemisphere and its inverted copy on the lower one, which should have no influence on the bulk phase (a similar argument was used in Ref. 11). The lower panel illustrates how this can be done for \mathbb{Z} -type 0D defects, for example in class BDI. This class has chiral symmetry and the zero modes can be assigned a definite chirality depending on whether they correspond to the \pm chirality eigenvalue such that the total chirality over the whole surface vanishes (in a 1D BDI wire, chirality distinguishes the zero mode at the two endpoints such that the two modes at the same endpoint do not hybridize but two modes belonging to different endpoints can gap out by hybridizing). Defects of opposite chirality can be brought together and annihilated as shown in the figure. This is equivalent to adding a BDI Majorana chain and its inverted copy to the surface.

The complete classification of inversion-protected k -th order TI/TSC in a given symmetry class in a given dimension d is given in Table I. As anticipated, the classification depends only on the dimensionality of the surface states $d - k$ and is always either 0 or \mathbb{Z}_2 . In addition, it turns out that the existence of higher-order TIs/TSCs in a given dimension and symmetry class requires imposing some constraints on the commutation/anticommutation relations between inversion and the local symmetries \mathcal{T} , \mathcal{P} , and \mathcal{S} , which will be derived in Sec. IV. This information is provided in Table I via the superscripts for \mathbb{Z}_2 , which indicate commutation (+) or anticommutation (-) relations between inversion symmetry and \mathcal{T} , \mathcal{P} , or \mathcal{S} (when present) for which a higher-order TI/TSC is possible. When the three symmetries \mathcal{T} , \mathcal{P} , or \mathcal{S} are present, we specify the commutation/anticommutation sign for time-reversal followed by that for particle-hole (we leave out the sign for chiral symmetry which is fixed by these two). Inversion is assumed to square to $+1$. The case of $\mathcal{I}^2 = -1$, which is relevant for example for inversion symmetry for spinful electrons in strictly 2D systems, is obtained by replacing $\mathcal{I} \rightarrow i\mathcal{I}$. This replacement changes the commutation/anticommutation sign

for the anti-unitary symmetries \mathcal{T} and \mathcal{P} but leaves the sign for \mathcal{S} unchanged.

III. PHYSICAL REALIZATIONS

A. Higher-order topological insulators

In this section, we consider examples of higher-order TIs. According to Table I, third-order TIs (classes A, AI or AII) are impossible in 3D, whereas second-order ones are only possible in 3D in the presence or absence of spinful TRS $\mathcal{T}^2 = -1$ corresponding to classes AII or A, respectively. In class A, this can be implemented by applying magnetic field (which breaks time-reversal but preserves inversion) to an inversion-symmetric time-reversal invariant 3D TI. To see this, let us consider the Hamiltonian for a 3D TI

$$\mathcal{H} = (\sin k_x \sigma_x + \sin k_y \sigma_y + \sin k_z \sigma_z) \tau_x - (3 - \lambda - \cos k_x - \cos k_y - \cos k_z) \sigma_0 \tau_z, \quad \lambda = 1. \quad (1)$$

Here, τ and σ denote the Pauli matrices in the orbital and spin spaces, respectively. The Hamiltonian (1) is invariant under inversion and time-reversal symmetries given respectively by $\mathcal{I} = \sigma_0 \tau_z$ and $\mathcal{T} = i \sigma_y \tau_0 \mathcal{K}$ (\mathcal{K} here indicates complex conjugation as usual).

Next, we place the system on some compact inversion-symmetric manifold in 3D (open boundary conditions in all directions). The derivation of the surface theory follows the standard procedure³⁹ by introducing a spatial dependence in the mass parameter $\lambda \rightarrow \lambda_t$, where t denotes the distance from the surface along the perpendicular direction. The surface is defined such that $\lambda_0 = 0$ and $\lambda_t \rightarrow \pm 1$ quickly away from the surface with the interior (exterior) of the sample corresponding to $+1$ (-1). We next linearize the Hamiltonian by expanding in small momenta around the Γ point and consider it close to the surface

$$\mathcal{H} = \boldsymbol{\sigma} \cdot \mathbf{k}_S \tau_x + [-i \boldsymbol{\sigma} \cdot \mathbf{n}_r \tau_x \partial_t + \lambda_t \sigma_0 \tau_z]. \quad (2)$$

Here, \mathbf{n}_r indicates the normal to the surface at point \mathbf{r} , satisfying $\mathbf{n}_{-\mathbf{r}} = -\mathbf{n}_r$ and \mathbf{k}_S is the momentum parallel to the surface (we assume the surface is a smooth manifold so that the surface momentum at a given by point can be defined as a vector in the tangent space at this point). We now look for the eigenstates ψ_{t, \mathbf{k}_S} of (2) that are localized close to the surface. These are fixed by the requirements that they decay fast enough away from the surface and are annihilated by the term between square brackets in (2) to be

$$\psi_{t, \mathbf{k}_S} = e^{\int_0^t dt' \lambda_{t'}} P \psi_{\mathbf{k}_S}, \quad P = \frac{1}{2} (1 - \mathbf{n}_r \cdot \boldsymbol{\sigma} \tau_y). \quad (3)$$

Here, P denotes the surface projection operator¹⁶, which can

be simplified by rotating to a basis where it is diagonal using

$$U_r = \exp\left(i \frac{\pi}{4} \tau_x \mathbf{n}_r \cdot \boldsymbol{\sigma}\right) \Rightarrow U_r^\dagger P U_r = \frac{1}{2} (1 - \tau_z \sigma_0). \quad (4)$$

We can now introduce the 4×2 matrix $p = (0, \sigma_0)^T$ which acts on a 4×4 matrix in the τ and σ space to pick up the 2×2 block corresponding to the non-zero eigenvalue of the rotated projector. The surface Hamiltonian can then be explicitly obtained as

$$h = p^T U_r^\dagger \tau_x \boldsymbol{\sigma} \cdot \mathbf{k} U_r p = p^T i \tau_0 (\boldsymbol{\sigma} \cdot \mathbf{k}_S) (\mathbf{n} \cdot \boldsymbol{\sigma}) p = -(\mathbf{k}_S \times \mathbf{n}) \cdot \boldsymbol{\sigma} = -(\mathbf{k} \times \mathbf{n}) \cdot \boldsymbol{\sigma}, \quad (5)$$

where we used the fact that $\mathbf{n} \times \mathbf{n} = 0$ in the last line to replace the surface momentum \mathbf{k}_S by the total momentum $\mathbf{k} = -i \nabla$. The symmetry action on the surface can be likewise deduced from its bulk action by the use of the projector (3) and basis rotation (4). Time-reversal symmetry acts on the surface degrees of freedom as

$$\mathcal{T}_S = p^T U_r^\dagger i \sigma_y \tau_0 \mathcal{K} U_r p = i \sigma_y \mathcal{K}, \quad (6)$$

which is the same as its action in the bulk. Inversion symmetry acts by mapping \mathbf{r} to $-\mathbf{r}$ and flipping the momentum \mathbf{k} and is represented on the surface by

$$\mathcal{I}_S = p^T U_r^\dagger \sigma_0 \tau_z U_r p = -\sigma_0. \quad (7)$$

We notice that, in principle, the symmetry action on the surface could depend on the point \mathbf{r} , as we will see in the next section, although this is not the case here.

We now allow for inversion-symmetric TRS-breaking mass terms, which can be achieved by applying a magnetic field. The only possible such term has the form $m_r \mathbf{n} \cdot \boldsymbol{\sigma}$ (this can be obtained as the surface projection of the bulk mass term $m_r \tau_y$). Inversion symmetry requires m_r to satisfy $m_{-\mathbf{r}} = -m_r$. As a result, this mass term has to vanish as we go between any point and its image under inversion along any curve, which in turn implies the existence of a 1D inversion-symmetric curve on which the mass term vanishes. Such 1D curve will host a chiral gapless mode analogous to the edge modes in a quantum Hall sample. The TRS-breaking mass term $m_r \mathbf{n} \cdot \boldsymbol{\sigma}$ can be identified as a Zeeman term resulting from applying a uniform magnetic field, with m_r being proportional to the field component normal to the surface. The curve along which the mass term vanishes corresponds to the region where the magnetic field is tangent to the surface and thus can be gauged away. Such a phase was studied before in Ref. 23.

In a cubic sample, the mass term is not expected to change along any face of the cube, thus we expect the chiral 1D mode to propagate along the edges or ‘‘hinges’’ of the sample. When the applied field is not parallel to any face, there are four possible configurations of inversion-symmetric edges where the modes can propagate, shown in Fig. 3 (for each configuration, the chiral mode can propagate in either direction), depending on the direction of the applied field. The Hamiltonian is expected to be gapless at edges where the field is tangent to the

TABLE I. **Classification of higher-order TIs/TSCs protected by inversion symmetry.** The first column s indicates the Bott label for the complex and real classes, the second column gives the AZ (or Cartan) label, and the next three columns indicate the presence (± 1) or absence (0) of time-reversal and particle-hole symmetries distinguishing the cases of $\mathcal{T}^2, \mathcal{P}^2 = \pm 1$ as well as the presence (1) or absence (0) of chiral symmetry $\mathcal{S} = \mathcal{TP}$. The next 8 columns give the classification of inversion-protected k -th order TI/TSC in d dimensions, which depends only on $D = d - k + 1$ ($k = 1$ corresponds to standard TIs/TSCs). The superscripts to the \mathbb{Z}_2 entries indicate the commutation properties of the inversion symmetry with the local symmetries \mathcal{T}, \mathcal{P} and \mathcal{S} (when present) for which the non-trivial phase is possible. For class AIII, the superscript $\sigma_S = \pm$ is defined as $\mathcal{S}^{-1}\mathcal{I}\mathcal{S} = \sigma_S\mathcal{I}$. For real classes with a single antiunitary symmetry $\mathcal{A} = \mathcal{T}, \mathcal{P}$ (AI, D, AII, C), the superscript $\sigma_A = \pm$ is similarly defined as $\mathcal{A}^{-1}\mathcal{I}\mathcal{A} = \sigma_A\mathcal{I}$. For real classes with both \mathcal{T} and \mathcal{P} symmetries (BDI, DIII, CII, CI), the two superscripts $\sigma_{\mathcal{T}, \mathcal{P}} = \pm$ are defined as $\mathcal{T}^{-1}\mathcal{I}\mathcal{T} = \sigma_{\mathcal{T}}\mathcal{I}$ and $\mathcal{P}^{-1}\mathcal{I}\mathcal{P} = \sigma_{\mathcal{P}}\mathcal{I}$, respectively ($\sigma_{\mathcal{T}}$ always comes first).

Symmetry				$D = d - k + 1$								
s	AZ class	\mathcal{T}^2	\mathcal{P}^2	\mathcal{S}^2	0	1	2	3	4	5	6	7
0	A	0	0	0	\mathbb{Z}_2	0	\mathbb{Z}_2	0	\mathbb{Z}_2	0	\mathbb{Z}_2	0
1	AIII	0	0	1	0	\mathbb{Z}_2^-	0	\mathbb{Z}_2^-	0	\mathbb{Z}_2^-	0	\mathbb{Z}_2^-
0	AI	1	0	0	\mathbb{Z}_2^+	0	0	0	$\mathbb{Z}_2^{+,-}$	0	$\mathbb{Z}_2^{+,-}$	\mathbb{Z}_2^+
1	BDI	1	1	1	$\mathbb{Z}_2^{+,-,++}$	\mathbb{Z}_2^{+-}	0	0	0	$\mathbb{Z}_2^{+,-,+}$	0	$\mathbb{Z}_2^{+,-,++,-+}$
2	D	0	1	0	$\mathbb{Z}_2^{+,-}$	\mathbb{Z}_2^-	\mathbb{Z}_2^-	0	0	0	$\mathbb{Z}_2^{+,-}$	0
3	DIII	-1	1	1	0	$\mathbb{Z}_2^{+,-,-,-,+}$	$\mathbb{Z}_2^{+,-,-}$	\mathbb{Z}_2^-	0	0	0	$\mathbb{Z}_2^{+,-,-}$
4	AII	-1	0	0	$\mathbb{Z}_2^{+,-}$	0	$\mathbb{Z}_2^{+,-}$	\mathbb{Z}_2^+	\mathbb{Z}_2^+	0	0	0
5	CII	-1	-1	1	0	$\mathbb{Z}_2^{+,-,+}$	0	$\mathbb{Z}_2^{+,-,++,-+}$	$\mathbb{Z}_2^{+,-,+}$	\mathbb{Z}_2^-	0	0
6	C	0	-1	0	0	0	$\mathbb{Z}_2^{+,-}$	0	$\mathbb{Z}_2^{+,-}$	\mathbb{Z}_2^-	\mathbb{Z}_2^-	0
7	CI	1	-1	1	0	0	0	$\mathbb{Z}_2^{+,-,+}$	0	$\mathbb{Z}_2^{+,-,-,-,+}$	$\mathbb{Z}_2^{+,-,-}$	\mathbb{Z}_2^+

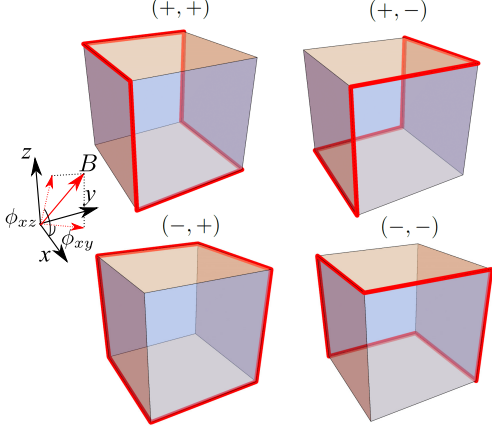


FIG. 3. Illustration of the pattern of surface states obtained by applying a magnetic field to a cubic sample of a time-reversal symmetric 3D TI. The four possible patterns correspond to the four possible values $(\text{sgn} \tan \phi_{xy}, \text{sgn} \tan \phi_{xz}) = (\pm, \pm)$, where ϕ_{xy} and ϕ_{xz} correspond to the angle between the x -axis and the projection of the field on the x - y plane and the x - z plane, respectively.

surface so that it can be gauged away. This leads to the dependence of the edge modes on the applied field schematically illustrated in Fig. 3, where the four possible configurations correspond to the values $(\text{sgn} \tan \phi_{xy}, \text{sgn} \tan \phi_{xz}) = (\pm, \pm)$. Here, ϕ_{xy} and ϕ_{xz} correspond to the angle between the x -axis and the projection of the field on the x - y plane and the x - z plane, respectively.

A time-reversal symmetric variant of this phase can be achieved by “stacking” two 3D TIs together as was shown in

Refs. 16 and 40. This can be seen by observing that a time-reversal-symmetric mass term can be added in a system consisting of two copies of the surface Hamiltonian (5), which is consistent with the fact that a 3D TI have a \mathbb{Z}_2 classification. Such mass term has the form $m_r \mathbf{n} \cdot \boldsymbol{\sigma} \gamma_y$ (γ are the Pauli matrices in the space of the two copies) and, in the presence of inversion, it will necessarily satisfy $m_{-r} = -m_r$. As a result, it will vanish along an inversion-symmetric 1D curve on the surface, which will host a propagating helical gapless mode similar to the edge of a quantum spin-Hall sample. This state can be thought of as a sum of the broken TRS case considered above and its time-reversed copy¹⁵.

B. Higher-order topological superconductors

1. Inversion symmetry in Bogoliubov-de Gennes Hamiltonians

Before discussing concrete physical realization for higher-order TSCs protected by inversion, it is instructive to review how inversion symmetry is implemented in Bogoliubov-de Gennes (BdG) Hamiltonians, which describe superconductors. A BdG Hamiltonian is given by

$$H = \frac{1}{2} \sum_{\mathbf{k}} (\psi_{\mathbf{k}}^\dagger, \psi_{-\mathbf{k}}) \mathcal{H}_{\mathbf{k}} \begin{pmatrix} \psi_{\mathbf{k}} \\ \psi_{-\mathbf{k}}^\dagger \end{pmatrix}, \quad \mathcal{H}_{\mathbf{k}} = \begin{pmatrix} \Xi_{\mathbf{k}} & \Delta_{\mathbf{k}} \\ \Delta_{\mathbf{k}}^\dagger & -\Xi_{-\mathbf{k}}^T \end{pmatrix}, \quad (8)$$

with $\psi_{\mathbf{k}} = (c_{\mathbf{k},\uparrow}, c_{\mathbf{k},\downarrow})$, $\Xi_{\mathbf{k}}$ representing the single particle part and $\Delta_{\mathbf{k}}$ the pairing or gap function. The Hamiltonian $\mathcal{H}_{\mathbf{k}}$ satisfies the PHS $\tau_x \mathcal{H}_{\mathbf{k}}^* \tau_x = -\mathcal{H}_{-\mathbf{k}}$, with τ representing the Pauli matrices in the particle-hole (Nambu) space (notice

that we use τ in this section to indicate Nambu space unlike Sec. III A, where it indicated orbital space). For a centrosymmetric superconductor, the single particle part $\Xi_{\mathbf{k}}$ is invariant under inversion $\mathcal{I}^{-1}\Xi_{\mathbf{k}}\mathcal{I} = \Xi_{-\mathbf{k}}$. For the gap function $\Delta_{\mathbf{k}}$, the two possibilities $\Delta_{-\mathbf{k}} = \pm\Delta_{\mathbf{k}}$ are consistent with inversion symmetry and they correspond to even (+) or odd (-) parity superconductors. It should be noted that in a simple two band model without spin-orbit coupling, even (odd) parity corresponds to a singlet (triplet) superconductor, but this relation does not hold in more complicated models^{35–38}. Inversion symmetry \mathcal{I} can be promoted to a symmetry \mathcal{I}^τ of the full BdG Hamiltonian by extending it to the Nambu space as

$$\mathcal{I}^\tau = \begin{cases} \mathcal{I} \otimes \tau_0, & : \Delta_{-\mathbf{k}} = \Delta_{\mathbf{k}}, \\ \mathcal{I} \otimes \tau_z, & : \Delta_{-\mathbf{k}} = -\Delta_{\mathbf{k}}, \end{cases} \quad (9)$$

which commutes (anticommutes) with PHS for even (odd) parity when $\mathcal{I}^2 = 1$. We note that the form of inversion symmetry (9) in odd parity superconductors was previously derived in Refs. 35 and 36, which concluded that odd parity is required to obtain a time-reversal symmetric TSC in 3D. According to Table I, most of the physically relevant cases for higher-order TIs/TSCs, e.g. second- or third-order class D in two or three dimensions, can only be achieved when inversion anti-commutes with PHS, which, as we have just seen, corresponds to odd-parity superconductors.

2. Three dimensions

We now consider examples of higher-order TSCs in 3D. According to Table I, it is possible to have higher-order TSCs with 1D (second-order) or 0D (third-order) surface states in triplet superconductors ($\mathcal{P}^2 = +1$) with or without spinful TRS, corresponding to classes DIII and D, respectively. Our approach to constructing these phases follows the previous section by either combining two 3D TSCs such that their strong 3D topological invariant vanishes or applying a TRS-breaking perturbation to a time-reversal-symmetric TSC. In both cases, the surface can be gapped out by writing a mass term which will be forced by inversion to vanish on a line or a pair of points on the surface. Our starting point is a topological superconductor of class DIII (spinful TRS), which can be thought of as the superconducting analog of a 3D strong TI but which differs in the fact that it has a \mathbb{Z} , rather than \mathbb{Z}_2 , classification.

A topologically non-trivial state $\nu = \pm 1$ in class DIII describes the B -phase in liquid ^3He ^{7,24,41}. The low energy effective Hamiltonian can be obtained from the BdG Hamiltonian by substituting $\Delta_{\mathbf{k}} = \mathbf{k} \cdot \boldsymbol{\sigma}(i\sigma_y)$ and $\Xi_{\mathbf{k}} = \lambda$ leading to

$$\mathcal{H}_\xi = \xi(-k_x\sigma_z\tau_x - k_y\tau_y + k_z\sigma_x\tau_x) + \lambda\sigma_0\tau_z, \quad \xi = \pm 1. \quad (10)$$

Here, τ indicates the Pauli matrices in the Nambu space as in Sec. III B 1 and $\boldsymbol{\sigma}$ indicates, as usual, the spin Pauli matrices. The Hamiltonian (10) is invariant under TRS $\mathcal{T} = \sigma_y\tau_0\mathcal{K}$, PHS $\mathcal{P} = \sigma_0\tau_x\mathcal{K}$, and consequently the chiral symmetry $\mathcal{S} = \sigma_y\tau_x$. It is also invariant under inversion symmetry im-

plemented as $\mathcal{I} = \sigma_0\tau_z$, which commutes with \mathcal{T} , but anti-commutes with \mathcal{P} . This is consistent with Table I and also with the discussion of Sec. III B 1 about inversion symmetry in odd-parity superconductors. Here, $\xi = \pm 1$ corresponds to phases with different topological indices $\nu = \pm 1$ and λ gives the negative of the chemical potential at $\mathbf{k} = 0$ (we assume that the single-particle dispersion depends weakly on \mathbf{k} close to $\mathbf{k} = 0$).

We will find it more convenient to perform the basis rotation

$$\mathcal{H}_\xi \rightarrow V^\dagger \mathcal{H}_\xi V, \quad V = e^{i\frac{\pi}{4}\sigma_y(\tau_z - \tau_0)}. \quad (11)$$

In the new basis, the Hamiltonian (10) becomes

$$\mathcal{H}_\xi = \xi \mathbf{k} \cdot \boldsymbol{\sigma} \tau_x + \lambda \sigma_0 \tau_z, \quad (12)$$

which has the same form as (2). Inversion and TRS are unaffected by the change of basis, while PHS and chiral symmetry are given in the new basis by $\mathcal{P} = \sigma_y\tau_y\mathcal{K}$ and $\mathcal{S} = \sigma_0\tau_y$, respectively.

The surface theory is derived as in Sec. III A using the rotation U_r defined in (4) followed by the projection

$$p_\xi = \begin{cases} (0, \sigma_0)^T & : \xi = +, \\ (\sigma_0, 0)^T & : \xi = -, \end{cases} \quad (13)$$

leading to the surface Hamiltonian

$$h_\xi = -\xi(\mathbf{k} \times \mathbf{n}_r) \cdot \boldsymbol{\sigma}. \quad (14)$$

One major subtlety in this case is the following: whereas the surface implementation of TRS and inversion, given respectively by $\mathcal{T}_S = \sigma_y\mathcal{K}$ and $\mathcal{I}_S = -\xi\sigma_0$, is independent on \mathbf{r} , the implementation of PHS (and consequently chiral symmetry) does depend on the point \mathbf{r} on the surface. It is easier to see this from the surface form of \mathcal{S} which is given by

$$\mathcal{S}_S = p_\xi^T U_r^\dagger \mathcal{S} U_r p_\xi = p_\xi^T \mathcal{S} U_r^2 p_\xi = p_\xi^T \mathbf{n} \cdot \boldsymbol{\sigma} \tau_z p_\xi = -\xi \mathbf{n} \cdot \boldsymbol{\sigma} \quad (15)$$

It follows that $\mathcal{P}_S = -\xi \mathbf{n} \cdot \boldsymbol{\sigma} \sigma_y \mathcal{K}$. The requirement of anticommutation with \mathcal{S}_S forbids any possible mass term even when we consider several copies of (14) with the same ξ , reflecting the \mathbb{Z} classification.

Let us now combine two copies of the Hamiltonian (12) with opposite topological index $\mathcal{H}_+ \oplus \mathcal{H}_-$ and consider the surface theory, which we can write more explicitly by introducing the Pauli matrices $\boldsymbol{\gamma}$ in the space of the two copies as

$$h = -(\mathbf{k} \times \mathbf{n}_r) \cdot \boldsymbol{\sigma} \boldsymbol{\gamma}_z. \quad (16)$$

Here, TRS, PHS, and inversion are implemented as $\mathcal{T}_S = \sigma_y\mathcal{K}$, $\mathcal{P}_S = -\boldsymbol{\gamma}_z \mathbf{n} \cdot \boldsymbol{\sigma} \sigma_y \mathcal{K}$, and $\mathcal{I} = -\boldsymbol{\gamma}_z$, respectively. Due to the vanishing strong index, we can write a mass term $m_r \boldsymbol{\gamma}_x$ which is invariant under TRS and PHS. Inversion implies $m_{-\mathbf{r}} = -m_r$ leading to a single helical 1D Majorana surface mode propagating along the inversion-symmetric 1D curve where the mass vanishes. This phase is the superconducting analog of the doubled strong TI discussed in the previous section (also in Refs. 15, 16, and 40) and it implements a

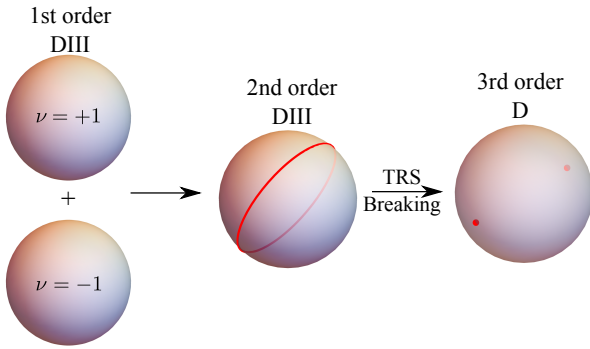


FIG. 4. Schematic illustration of the construction of a third-order TSC with two corner states in 3D. The first stage involves combining two (first-order) 3D time-reversal symmetric TSCs (class DIII) with opposite topological index $\nu = \pm 1$ leading to a second-order time-reversal symmetric TSC (class DIII) with a helical 1D mode. The second stage involves applying a TRS-breaking perturbation leading to a third-order TSC with broken TRS (class D) with a pair of Majorana zero modes at two antipodal points.

second-order TSC in class DIII. Similarly, we can implement a second-order TSC in class D by applying a magnetic field to the surface Hamiltonian of a single copy of the DIII Hamiltonian (14). In this case, the only mass term consistent with preserved PHS and broken TRS is $m_{\mathbf{r}} \mathbf{n} \cdot \boldsymbol{\sigma}$. This mass term is again required by inversion symmetry to vanish along a 1D inversion-symmetric curve which will host a propagating chiral Majorana mode. This phase can be realized by applying a magnetic field to topological superfluid $^3\text{He-B}$ and it was previously studied in Ref. 24.

We can now build a third-order TSC in 3D with corner modes by applying a TRS-breaking perturbation to the time-reversal invariant second-order TSC constructed above. The only possible PHS-preserving and TRS-breaking mass term that can be added to gap out the 1D helical mode on the surface is given by $\tilde{m}_{\mathbf{r}} \gamma_y$ which satisfies $\tilde{m}_{-\mathbf{r}} = -\tilde{m}_{\mathbf{r}}$ due to inversion. This means that the 1D helical surface mode can be gapped out except at two antipodal points where both surface mass terms $m_{\mathbf{r}}$ and $\tilde{m}_{\mathbf{r}}$ have to vanish. These two points resemble magnetic vortices (the two mass terms are similar to the real and imaginary part of a gap function) and they will host a Majorana mode each, similar to the vortices in a $p_x \pm ip_y$ superconductor. The construction is schematically illustrated in Fig. 4.

3. Two dimensions

In analogy to the previous two sections, we can build a second-order 2D TSC in class D by applying a TRS-breaking perturbation to a 2D time-reversal-symmetric TSC (class DIII). Such a 2D TSC can be implemented as a p_x (or p_y) wave superconductor, as a superposition of a $(p_x + ip_y)$ -superconductor and its time-reversed copy⁷, or by proximity coupling the surface of a 3D TI to a superconductor as shown by Fu and Kane⁴². Although these implementations all corre-

spond to the AZ class DIII, the first two differ from the last one in the commutation relations between inversion and particle-hole symmetries. Whereas a p -wave superconductor is an odd parity superconductor with inversion anti-commuting (commuting) with PHS for $\mathcal{I}^2 = +1$ ($\mathcal{I}^2 = -1$), a Fu-Kane superconductor is typically constructed by proximity coupling to an s -wave superconductor where inversion commutes (anti-commutes) with PHS for $\mathcal{I}^2 = +1$ ($\mathcal{I}^2 = -1$). Furthermore, both implementations $\mathcal{I}^2 = +1$ and $\mathcal{I}^2 = -1$ are possible in 2D. The former corresponds to 3D spatial inversion restricted to the 2D plane (which also flips the normal to the plane), which is relevant for example in a layered material with an inversion center in the middle, while the latter represents strictly 2D inversion which is equivalent to two-fold rotation about the axis perpendicular to the plane. According to Table I, a second-order TSC in class D is only possible when inversion anti-commutes (commutes) with PHS for $\mathcal{I}^2 = +1$ ($\mathcal{I}^2 = -1$), which means that it is only possible starting from a p -wave superconductor either in a layered (quasi-2D) setting with 3D inversion or in a strictly 2D system with C_2 symmetry. The two cases are related by the replacement $\mathcal{I}_{2D} = i\mathcal{I}_{3D}$, and in the following we will only focus on the layered (quasi-2D) setting where inversion satisfies $\mathcal{I}^2 = 1$.

We start with the Hamiltonian describing a superposition of $p_x + ip_y$ and $p_x - ip_y$ superconductors. Using the gap function $\Delta(\mathbf{k}) = -\sigma_z k_x + i\sigma_0 k_y$, we can write this Hamiltonian as

$$\mathcal{H} = -k_x \sigma_z \tau_x - k_y \tau_y + \lambda \tau_z. \quad (17)$$

Here, we assume the \mathbf{k} -dependence of the single particle dispersion is weak close to 0 and replace it by a constant λ . This Hamiltonian has PHS given by $\mathcal{P} = \sigma_0 \tau_x \mathcal{K}$, TRS given by $\mathcal{T} = \sigma_y \tau_0 \mathcal{K}$, and inversion symmetry given by $\mathcal{I} = \sigma_0 \tau_z$.

The combination of TRS and PHS prohibits any mass term. The only allowed TRS-breaking mass term is $m_{\mathbf{r}} \sigma_y \tau_x$, which satisfies $m_{-\mathbf{r}} = -m_{\mathbf{r}}$ due to inversion. As a result, it has to vanish at least twice at two inversion-related points on any given compact inversion-symmetric edge. We can see this more explicitly by writing the edge theory following the same procedures as in Secs. III A and III B 2 leading to

$$h = -k_S \sigma_z, \quad (18)$$

where k_S is the momentum parallel to the edge. The edge implementation of TRS, PHS and inversion is given respectively by $\mathcal{T}_S = \sigma_y \mathcal{K}$, $\mathcal{P}_S = -\mathbf{n}_{\mathbf{r}} \cdot \boldsymbol{\sigma} \sigma_y \mathcal{K}$, and $\mathcal{I}_S = \sigma_0$, where $\mathbf{n}_{\mathbf{r}}$ is the normal to the edge in the 2D plane. The only possible TRS-breaking surface mass term consistent with PHS is $m_{\mathbf{r}} \mathbf{n}_{\mathbf{r}} \cdot \boldsymbol{\sigma}$ which we can identify as a Zeeman term for an in-plane field. The field will fail to gap out the Hamiltonian at the two points where it is tangent to the edge, which will host a single Majorana mode each. Using this phase, we can also build a second-order 2D TSC in classes BDI or DIII by adding it to a time-reversed copy of itself with spinful or spinless TRS, respectively.

IV. LAYER CONSTRUCTION

To establish the conditions in Table I, we make use of the layer construction introduced in Refs. 28, 29, and 43 to study topological phases protected by point group symmetries. Before presenting the general argument, we will first illustrate it using the example of a second-order 3D TI with unbroken TRS (class AII). We first note that being a symmetry protected topological phase means that it becomes trivial in the absence of inversion symmetry. If we now consider an inversion symmetric plane (i.e. one that contains the inversion center), it will divide the 3D space into two regions mapped to each other under inversion. Each region separately does not have inversion symmetry and is therefore trivial, implying that the non-triviality of the phase is only encoded in the 2D plane. To get 1D helical modes, this 2D plane needs to be a strong TI, which in this case is just a quantum-spin Hall (QSH) system. The same argument can be applied to construct a third-order TI/TSC with 0D states, which is not possible in class AII but possible, for instance, in the superconducting classes D or BDI. In this case, we have to carry out the procedure further by assuming that the 2D layer itself hosts an inversion-symmetry protected phase, rather than a strong TI/TSC, and split it in half via a line through the inversion center. If this line hosts a 1D strong TI/TSC, e.g. an SSH chain, then we get a 3D third-order TSC. This argument can be generalized to relate any inversion-protected k -th order TI/TSC in d dimensions to a $(d-k+1)$ -dimensional inversion-symmetric strong TI/TSC.

The construction of the previous paragraph can also be reversed. Starting with an inversion-symmetric 2D QSH layer, we can build a second-order 3D TI in class AII by stacking 2D layers. To ensure that inversion symmetry is preserved, each step of the stacking consists of adjoining the system with a 2D layer (which can either be QSH or trivial insulating layers) and its copy under inversion. The procedure is shown schematically in Fig. IV, where we assumed for simplicity that all layers are QSHs which are arranged such that they are equally spaced along the stacking direction. The resulting system is a 3D weak TI, whose gapless surface states are protected by translation. Breaking translation while preserving inversion will gap out the surface states except for a single 1D helical edge mode living on an inversion-symmetric curve.

In general, the construction of an inversion-protected k -th order TI/TSC in d dimensions starts with an inversion-symmetric $(d-k+1)$ -dimensional strong TI/TSC as a building block and successively adjoins it with $(d-k+1)$ -dimensional blocks and their inverted copies. This suggests that the problem of classifying inversion-protected higher-order TIs/TSCs reduces to the problem of classifying inversion-symmetric strong (first-order) TIs/TSCs, i.e. those which are compatible with inversion symmetry. It should be noted, however, that not every lower-dimensional TI/TSC compatible with the symmetry would lead to a unique higher-dimensional higher-order TI/TSC. The reason is that two lower-dimensional strong phases related by the adjoining operation, which adds to the system a “layer” and its copy under inversion, lead to the same higher-dimensional phase and should thus be identified²⁸.

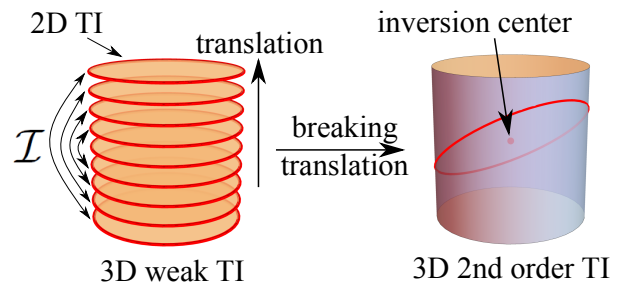


FIG. 5. Schematic illustration of the layer construction. Here, we can construct a second-order TI in 3D starting with a 2D strong (first order) TI and adjoining it with 2D layers and their images under inversion. We choose here to do it such that the resulting system has translational symmetry along the stacking direction, thus realizing a 3D weak TI. Breaking the translational symmetry while keeping inversion leads to a second-order TI with a single 1D mode which lives on some inversion-symmetric curve on the surface.

The resulting classification criterion for higher-order TI/TSC is the following:

Inversion-protected k -th order TIs/TSCs in d dimensions are in one-to-one correspondence with minimal inversion-symmetric strong (first-order) TIs/TSCs in $d-k+1$ dimensions. A minimal TI/TSC is one which cannot be written as a sum of a TI/TSC and its copy under inversion.

The aforementioned criterion leads immediately to the anticipated \mathbb{Z}_2 classification since the sum of two inversion-symmetric strong TIs/TSCs can always be thought of as a sum of a strong TI/TSC and its copy under inversion, which is equivalent to a trivial system under the adjoining operation. We can also easily understand some of the constraints in Table I. For instance, inversion symmetry is always required to anti-commute with the chiral symmetry in order for higher-order TIs to be possible in class AIII. This can be easily seen from the fact that strong TIs in class AIII are classified with an integer winding number in odd dimensions d given by^{8,27} $\sim \int \text{tr} \mathcal{S} (\mathcal{H}^{-1} d\mathcal{H})^{2n+1}$, which is even (odd) under inversion when it anti-commutes (commutes) with the chiral symmetry \mathcal{S} . Therefore, a non-vanishing winding number cannot be consistent with an inversion symmetry which commutes with \mathcal{S} .

To establish the classification of Table I, we need to classify all minimal inversion-symmetric strong TIs/TSCs. Noting that the Hamiltonian of any minimal strong TI can be smoothly deformed to a Dirac Hamiltonian (DH), this problem reduces to the simple problem of classifying possible inversion operators in a DH.

Let us now first review the DH description for strong TIs/TSCs. The ten AZ symmetry classes are divided into two complex and eight real classes. The former includes classes which do not possess any antiunitary symmetry relating the first quantized Hamiltonian to its complex conjugate. These are unitary (A) and chiral unitary (AIII) classes which are denoted by the complex s_c parameter $s_c = 0$ and $s_c = 1$ respectively (cf. Table I). Real classes include the remaining eight classes which are labeled by the parameter $s_r = 0, \dots, 7$ as shown in Table I. A TI/TSC with a \mathbb{Z} classification is pos-

sible in the complex classes whenever $s_c - d = 0 \pmod 2$. The \mathbb{Z} invariant is a Chern number in even dimensions and a winding number in odd dimensions. Examples include the SSH chain in 1D⁴⁴ ($s_c = 1$) and the quantum Hall effect in 2D^{45,46} ($s_c = 0$). For real classes, there are four series of TIs/TSCs given by $s_r - d = 0, 1, 2, 4 \pmod 8$. The series $s_r - d = 0 \pmod 8$ has a \mathbb{Z} invariant given by a Chern number in even dimensions and a winding number in odd dimensions. It includes topological $p_x \pm ip_y$ TSCs in 2D^{7,30} ($s_r = 2$) and topological superfluid ³He-B in 3D^{7,24,41} ($s_r = 3$). The first and second descendant series are given respectively by $s_r - d = 1, 2 \pmod 8$ and they both have \mathbb{Z}_2 classification. An example of the former is the 3D time-reversal-symmetric TI^{47,48} ($s_r = 4$) and of the latter is the quantum-spin Hall insulator in 2D⁴⁹⁻⁵¹ ($s_r = 4$). Finally, there is the $s_r - d = 4 \pmod 8$ series which has a $2\mathbb{Z}$ classification, meaning that the Chern number (for even dimensions) or the winding number (for odd dimensions) is always even⁶⁻⁸.

A DH for the minimal strong TI/TSC can be written in all cases as

$$\mathcal{H}_{\mathbf{k}} = \sum_{i=1}^d \Gamma_i \sin k_i - \mathcal{M}(d-1 - \sum_{i=1}^d \cos k_i). \quad (19)$$

Here, Γ_i denotes a set of Dirac matrices satisfying the Clifford algebra $\{\Gamma_i, \Gamma_j\} = 2\delta_{ij}$ with $i, j = 1, \dots, 2n+1$. Only n of these Γ matrices are imaginary and we choose these to be the even ones. The Dirac mass \mathcal{M} always satisfies $\mathcal{M}^2 = 1$ and $\{\mathcal{M}, \Gamma_i\} = 0$ for $i = 1, \dots, d$. Time-reversal, particle-hole, chiral, and inversion symmetry act on the Hamiltonian as

$$\begin{aligned} \mathcal{T}^{-1} \mathcal{H}_{\mathbf{k}}^* \mathcal{T} &= \mathcal{H}_{-\mathbf{k}}, & \mathcal{P}^{-1} \mathcal{H}_{\mathbf{k}}^* \mathcal{P} &= -\mathcal{H}_{-\mathbf{k}} \\ \mathcal{S}^{-1} \mathcal{H}_{\mathbf{k}} \mathcal{S} &= -\mathcal{H}_{\mathbf{k}}, & \mathcal{I}^{-1} \mathcal{H}_{\mathbf{k}} \mathcal{I} &= \mathcal{H}_{-\mathbf{k}}. \end{aligned} \quad (20)$$

The possible choices of the mass term \mathcal{M} for different symmetry classes in different dimensions are given in Table II, where strong TIs/TSCs correspond to $k = 1$ (first-order). The anti-unitary operator \mathcal{A} used in the table is defined for $k = 1$ as

$$\mathcal{A} = \prod_{\substack{l=1 \\ l \text{ odd}}}^d \Gamma_l \mathcal{K}, \quad (21)$$

and it may commute (anti-commute) with the DH (19) depending on the choice of the mass term \mathcal{M} and the dimension, representing TRS (PHS). The 7th column in Table II provides all possible implementations of the inversion operator \mathcal{I} such that $\mathcal{I}^2 = 1$, $[\mathcal{I}, \mathcal{M}] = 0$, and $\{\mathcal{I}, \Gamma_i\} = 0$ for $i = 1, \dots, d$. The next three columns indicate whether it commutes (+) or anti-commutes (-) with \mathcal{T} , \mathcal{P} , and \mathcal{S} , thus establishing the classification in Table I.

V. MINIMAL MODEL FOR HIGHER-ORDER TOPOLOGICAL INSULATORS AND SUPERCONDUCTORS IN ARBITRARY DIMENSION

In this section, we provide a minimal model for k -th order TIs/TSCs in d spatial dimensions using Dirac Hamiltonians. The construction of the model relies on the observation that higher-order TIs/TSCs can be built by adding $k-1$ extra mass terms, which are odd under inversion, to the DH for a strong (first-order) TI/TSC (cf. Sec. III). Generically, these mass terms will simultaneously vanish at a $(d-k)$ -dimensional region on the surface, leading to $(d-k)$ -dimensional surface states. More explicitly, a DH describing a k -th order TI/TSC in d spatial dimensions for $s_c - d + k - 1 = 0 \pmod 2$ or $s_r - d + k - 1 = 0, 1, 2, 4 \pmod 8$ is given by

$$\begin{aligned} \mathcal{H} &= - \sum_{i=1}^d i \Gamma_i \partial_i + \sum_{j=1}^{k-1} m_{j,r} \Gamma_{d+j} + \lambda \mathcal{M} \\ &= -i \boldsymbol{\gamma} \cdot \boldsymbol{\nabla} + \mathbf{m}_r \cdot \boldsymbol{\alpha} + \lambda \mathcal{M}, \end{aligned} \quad (22)$$

where we introduced the vectors $\boldsymbol{\gamma}$, \mathbf{m} and $\boldsymbol{\alpha}$ defined as

$$\begin{aligned} \boldsymbol{\gamma} &= (\Gamma_1, \dots, \Gamma_d), & \boldsymbol{\alpha} &= (\Gamma_{d+1}, \dots, \Gamma_{d+k-1}), \\ \mathbf{m}_r &= (m_{1,r}, \dots, m_{k-1,r}). \end{aligned} \quad (23)$$

\mathcal{M} is given in Table II for different symmetry classes in different dimensions. The anti-unitary operator \mathcal{A} is defined as

$$\mathcal{A} = \prod_{\substack{l=1 \\ l \text{ odd}}}^d \Gamma_l \prod_{\substack{m=d+1 \\ m \text{ even}}}^{d+k-1} \Gamma_m \mathcal{K}, \quad (24)$$

and it corresponds to TRS or PHS depending on the symmetry class and the dimension as explained in Table II. The possible choices of the inversion symmetry operator are given by the 7th column of the table. It is constructed such that it anti-commutes with all Γ_l for $l = 1, \dots, d+k-1$ and commutes with \mathcal{M} . As a result, it enforces the condition $m_{j,-r} = -m_{j,r}$.

In order to see the type of surface states corresponding to the DH (22), we follow the same procedure of Sec. III and take λ to change from 1 inside the sample to -1 outside it across some inversion-symmetric surface. We then introduce the projection operators

$$P_{\pm} = \frac{1}{2}(1 \mp i \mathbf{n}_r \cdot \boldsymbol{\gamma} \mathcal{M}), \quad P_{\pm}^2 = P_{\pm}, \quad P_+ P_- = 0, \quad (25)$$

where \mathbf{n}_r is the normal to the surface at point r . Using the projector P_+ , the surface Hamiltonian can be obtained as

$$h = \tilde{\boldsymbol{\gamma}} \cdot \mathbf{k}_S + \mathbf{m}_r \cdot \tilde{\boldsymbol{\alpha}}, \quad \tilde{\boldsymbol{\gamma}} = P_+ \boldsymbol{\gamma} P_+, \quad \tilde{\boldsymbol{\alpha}} = P_+ \boldsymbol{\alpha} P_+, \quad (26)$$

where \mathbf{k}_S is the momentum tangent to the surface. The projector P_+ ensures that the momentum perpendicular to the surface drops out since

$$\mathbf{n}_r \cdot \tilde{\boldsymbol{\gamma}} = P_+ \mathbf{n}_r \cdot \boldsymbol{\gamma} P_+ = P_+ P_- \mathbf{n}_r \cdot \boldsymbol{\gamma} = 0, \quad (27)$$

which follows from the relation $P_+ \mathbf{n}_r \cdot \boldsymbol{\gamma} = \mathbf{n}_r \cdot \boldsymbol{\gamma} P_-$ (since \mathcal{M} anticommutes with $\mathbf{n}_r \cdot \boldsymbol{\gamma}$).

We now consider an orthonormal basis $\{e_i\}$ in the $(d-1)$ -dimensional plane tangent to the surface at a given point \mathbf{r} , i.e. $e_i \cdot e_j = \delta_{ij}$, and define $\tilde{\gamma}_i = e_i \cdot \tilde{\boldsymbol{\gamma}}$. It is easy to see that

$$\{\tilde{\gamma}_i, \tilde{\gamma}_j\} = 2\delta_{ij}P_+, \quad \{\tilde{\gamma}_i, \tilde{\alpha}_l\} = 0, \quad \{\tilde{\alpha}_l, \tilde{\alpha}_m\} = 2\delta_{lm}P_+, \quad (28)$$

for $i, j = 1, \dots, d-1$ and $l, m = 1, \dots, k-1$. This means that $\tilde{\gamma}_i$ and $\tilde{\alpha}_l$ form a Clifford algebra (of smaller dimension) once projected to the non-zero block of the projector P_+ and the surface Hamiltonian has the spectrum

$$\epsilon_{\mathbf{r}, \mathbf{k}_S} = \pm \sqrt{\mathbf{k}_S^2 + \mathbf{m}_r^2}, \quad (29)$$

which is gapless whenever all the masses $m_{j,\mathbf{r}}$ vanish. Each of them is odd under inversion $m_{j,-\mathbf{r}} = -m_{j,\mathbf{r}}$ and thus vanishes on a $(d-2)$ -dimensional region on the surface. It follows that they all simultaneously vanish at a $(d-k)$ -dimensional region on the surface, thus realizing a k -th order TI/TSC.

VI. DISCUSSION

We now make a few closing remarks regarding the stability of the phases considered in this work, its relation to other works, and the generalization of the analysis considered here for other spatial symmetries.

First, we note that, similar to other gapped topological phases of matter, the phases considered here are protected by the bulk gap. This means that symmetry-preserving perturbations that are small enough compared to the bulk gap will not be able to destroy the surface states. They can, however, move the surface states around as explained in the main text. We note also that the surface states are stable against inversion-breaking perturbations, e.g. disorder, provided they are small compared to the maximal value of the surface gap. The reason for this is that the local stability of the surface states relies only on the local symmetries \mathcal{T} , \mathcal{P} , and \mathcal{S} . Therefore, the only way to remove them is by deforming them all the way to a point, for example by bringing two corner states together or deforming a 1D surface state to a point. In summary, bulk gap provides protection against inversion-preserving perturbations, while surface gap provides protection against inversion-breaking perturbations. This conclusion is consistent with the numerical analysis of Ref. 12, which showed that the surface states in a mirror-protected second-order TIs/TSCs are stable against mirror-symmetry-breaking perturbations. Note, however, that perturbations which break the local symmetries \mathcal{T} , \mathcal{P} , and \mathcal{S} can generally destabilize the surface states even if they are very small.

Second, we reiterate here that we do not provide a classification of all TCIs protected by inversion, which was obtained using K-theory in Refs. 26 and 27. Instead, we classify the subset of these TCIs that host surface states. This subset is a

proper subset, which can be directly verified by comparing the classification obtained here (Table I) to the results obtained in Refs. 26 and 27 (note that Ref. 26 considered only the case where inversion symmetry commutes with all other symmetries). We stress that the states obtained in this work exhaust all possible surface states protected by inversion symmetry in the 10 AZ symmetry classes in any dimension. Unlike other spatial symmetries which leave some surface planes invariant, e.g. mirror symmetry, inversion does not leave any plane on the surface invariant. Therefore, inversion-protected surface states can only be observed by considering a sample with compact geometry with open boundary conditions in all directions, where the surface is considered as a whole.

Finally, we note that the method we used here, which combines a Dirac analysis with the layer construction used in Refs. 28, 29, and 52, can be readily generalized to any spatial symmetry and it does not require the knowledge of the full K-theory classification of the corresponding TCIs, which is only known for order-two symmetry operations²⁷. The method employed here was recently used to classify all possible surface states in TCIs with strong spin-orbit coupling (class AII) protected by any crystalline symmetry in the 230 space groups¹⁶. Although the extension of our results to include other spatial symmetries, e.g. rotations, is straightforward, the analysis is more complicated since special care is needed when considering points, lines, or planes on the surface which are left invariant by the symmetry. In addition, the existence of surface states may, in many cases, require unphysical commutation or anticommutation relations between time-reversal or particle-hole symmetries and the spatial symmetries. A careful investigation would then be required to separate the physically more relevant cases as we have done in this work. Furthermore, higher-order TIs/TSCs protected by symmetries with invariant planes (which includes all other point group symmetries apart from roto-inversion) can usually be understood in a more conventional way by studying possible surface states on these planes. Therefore, we choose to leave this question to future works.

Note added. After the completion of this work, the author became aware of two related studies: one considers second-order topological insulators and superconductors protected by order-two symmetries⁵³ and the other discusses a realization of a two-dimensional second-order topological superconductor⁵⁴ similar to the one considered in Sec. III B 3 of this work.

ACKNOWLEDGMENTS

The author would like to acknowledge stimulating discussions with P. W. Brouwer, M. Geier, A. P. Schnyder, H. C. Po, and A. Vishwanath. I am grateful to P. W. Brouwer for pointing out an error in an earlier version of this manuscript and for informing me of their related upcoming work⁵³ and to E. Locane for proofreading the manuscript.

- ¹ M. Franz and L. Molenkamp, eds., *Topological Insulators*, Contemporary Concepts of Condensed Matter Science, Vol. 6 (Elsevier, 2013).
- ² M. Z. Hasan and C. L. Kane, *Rev. Mod. Phys.* **82**, 3045 (2010).
- ³ J. Moore, *Nat. Phys.* **5**, 378 (2009).
- ⁴ X.-L. Qi and S.-C. Zhang, *Rev. Mod. Phys.* **83**, 1057 (2011).
- ⁵ A. Altland and M. R. Zirnbauer, *Phys. Rev. B* **55**, 1142 (1997).
- ⁶ A. Kitaev, in *AIP Conference Proceedings*, Vol. 1134 (AIP, 2009) pp. 22–30.
- ⁷ A. P. Schnyder, S. Ryu, A. Furusaki, and A. W. Ludwig, in *AIP Conference Proceedings*, Vol. 1134 (AIP, 2009) pp. 10–21.
- ⁸ S. Ryu, A. P. Schnyder, A. Furusaki, and A. W. W. Ludwig, *New J. Phys.* **12**, 065010 (2010).
- ⁹ L. Fu, *Phys. Rev. Lett.* **106**, 106802 (2011).
- ¹⁰ T. H. Hsieh, H. Lin, J. Liu, W. Duan, A. Bansil, and L. Fu, *Nature Communications* **3**, 982 EP (2012), article.
- ¹¹ F. Schindler, A. M. Cook, M. G. Vergniory, Z. Wang, S. S. Parkin, B. A. Bernevig, and T. Neupert, arXiv preprint arXiv:1708.03636 (2017).
- ¹² J. Langbehn, Y. Peng, L. Trifunovic, F. von Oppen, and P. W. Brouwer, arXiv preprint arXiv:1708.03640 (2017).
- ¹³ W. A. Benalcazar, B. A. Bernevig, and T. L. Hughes, *Science* **357**, 61 (2017).
- ¹⁴ Z. Song, Z. Fang, and C. Fang, arXiv preprint arXiv:1708.02952 (2017).
- ¹⁵ C. Fang and L. Fu, arXiv preprint arXiv:1709.01929 (2017).
- ¹⁶ E. Khalaf, H. C. Po, A. Vishwanath, and H. Watanabe, arXiv preprint arXiv:1711.11589 (2017).
- ¹⁷ W. A. Benalcazar, B. A. Bernevig, and T. L. Hughes, ArXiv e-prints (2017), arXiv:1708.04230.
- ¹⁸ M. Serra-Garcia, V. Peri, R. Süssstrunk, O. R. Bilal, T. Larsen, L. G. Villanueva, and S. D. Huber, *Nature*, EP (2018).
- ¹⁹ S. Imhof, C. Berger, F. Bayer, J. Brehm, L. Molenkamp, T. Kiessling, F. Schindler, C. H. Lee, M. Greiter, T. Neupert, *et al.*, arXiv preprint arXiv:1708.03647 (2017).
- ²⁰ C. W. Peterson, W. A. Benalcazar, T. L. Hughes, and G. Bahl, arXiv preprint arXiv:1710.03231 (2017).
- ²¹ M. Ezawa, *Phys. Rev. Lett.* **120**, 026801 (2018).
- ²² M. Ezawa, arXiv preprint arXiv:1801.00437 (2018).
- ²³ M. Sitte, A. Rosch, E. Altman, and L. Fritz, *Phys. Rev. Lett.* **108**, 126807 (2012).
- ²⁴ G. E. Volovik, *JETP Letters* **91**, 201 (2010).
- ²⁵ Y. Tanaka, Z. Ren, T. Sato, K. Nakayama, S. Souma, T. Takahashi, K. Segawa, and Y. Ando, *Nature Physics* **8**, 800 (2012).
- ²⁶ Y.-M. Lu and D.-H. Lee, arXiv preprint arXiv:1403.5558 (2014).
- ²⁷ K. Shiozaki and M. Sato, *Phys. Rev. B* **90**, 165114 (2014).
- ²⁸ H. Song, S.-J. Huang, L. Fu, and M. Hermele, *Phys. Rev. X* **7**, 011020 (2017).
- ²⁹ S.-J. Huang, H. Song, Y.-P. Huang, and M. Hermele, *Phys. Rev. B* **96**, 205106 (2017).
- ³⁰ N. Read and D. Green, *Phys. Rev. B* **61**, 10267 (2000).
- ³¹ D. A. Ivanov, *Phys. Rev. Lett.* **86**, 268 (2001).
- ³² J. C. Y. Teo and C. L. Kane, *Phys. Rev. B* **82**, 115120 (2010).
- ³³ Whenever we refer to a compact surface in this work, we implicitly assume it has genus 0, e.g. a sphere.
- ³⁴ A similar argument can be made for point group symmetries other than inversion. In that case, however, we need to be careful when we consider points/lines which are left invariant by the symmetry, where the spatial symmetry acts as an onsite unitary symmetry, possibly leading to a different effective symmetry class at these invariant regions.
- ³⁵ L. Fu and E. Berg, *Phys. Rev. Lett.* **105**, 097001 (2010).
- ³⁶ M. Sato, *Phys. Rev. B* **81**, 220504 (2010).
- ³⁷ Y. Ando and L. Fu, *Annual Review of Condensed Matter Physics* **6**, 361 (2015), <https://doi.org/10.1146/annurev-conmatphys-031214-014501>.
- ³⁸ M. Sato and Y. Ando, *Reports on Progress in Physics* **80**, 076501 (2017).
- ³⁹ R. Jackiw and C. Rebbi, *Phys. Rev. D* **13**, 3398 (1976).
- ⁴⁰ H. C. Po, A. Vishwanath, and H. Watanabe, *Nature Communications* **8**, 50 (2017).
- ⁴¹ G. E. Volovik, *The universe in a helium droplet*, Vol. 117 (Oxford University Press on Demand, 2003).
- ⁴² L. Fu and C. L. Kane, *Phys. Rev. Lett.* **100**, 096407 (2008).
- ⁴³ H. Isobe and L. Fu, *Phys. Rev. B* **92**, 081304 (2015).
- ⁴⁴ W. P. Su, J. R. Schrieffer, and A. J. Heeger, *Phys. Rev. Lett.* **42**, 1698 (1979).
- ⁴⁵ K. v. Klitzing, G. Dorda, and M. Pepper, *Phys. Rev. Lett.* **45**, 494 (1980).
- ⁴⁶ D. J. Thouless, M. Kohmoto, M. P. Nightingale, and M. den Nijs, *Phys. Rev. Lett.* **49**, 405 (1982).
- ⁴⁷ L. Fu, C. L. Kane, and E. J. Mele, *Phys. Rev. Lett.* **98**, 106803 (2007).
- ⁴⁸ J. E. Moore and L. Balents, *Phys. Rev. B* **75**, 121306 (2007).
- ⁴⁹ C. L. Kane and E. J. Mele, *Phys. Rev. Lett.* **95**, 226801 (2005).
- ⁵⁰ C. L. Kane and E. J. Mele, *Phys. Rev. Lett.* **95**, 146802 (2005).
- ⁵¹ B. A. Bernevig, T. L. Hughes, and S.-C. Zhang, *Science* **314**, 1757 (2006).
- ⁵² Z. Song, T. Zhang, Z. Fang, and C. Fang, arXiv preprint arXiv:1711.11049 (2017).
- ⁵³ M. Geier, L. Trifunovic, M. Hoskam, and P. W. Brouwer, arXiv preprint arXiv:1801.10053 (2018).
- ⁵⁴ X. Zhu, arXiv preprint arXiv:1802.00270 (2018).

TABLE II. **Data for the Dirac Hamiltonian description for higher-order TIs/TSCs.** The first column gives the AZ label for the five series of higher-order TIs/TSCs $s_c - D = 0 \pmod 2$ (complex) and $s_r - D = 0, 1, 2, 4 \pmod 8$ (real), with D given by $D = d - k + 1$ as in Table I. The third column gives the Dirac mass for the Hamiltonian (22) consistent with the given symmetry class and dimension. The next three columns provide the explicit implementation for time-reversal, particle-hole and chiral symmetries, in terms of the anti-unitary operator \mathcal{A} defined in (24). The 7th column gives all possible implementations of the inversion symmetry \mathcal{I} such that it satisfies $\mathcal{I}^2 = 1$, $[\mathcal{I}, \mathcal{M}] = 0$, and $\{\mathcal{I}, \Gamma_i\} = 0$ for $i = 1, \dots, d+k-1$. The last three columns give the commutation/anti-commutation sign of inversion with time-reversal, particle-hole and chiral symmetries defined as $\sigma_{\mathcal{T}} = \mathcal{I}\mathcal{T}^{-1}\mathcal{I}\mathcal{T}$, $\sigma_{\mathcal{P}} = \mathcal{I}\mathcal{P}^{-1}\mathcal{I}\mathcal{P}$, and $\sigma_{\mathcal{S}} = \mathcal{I}\mathcal{S}^{-1}\mathcal{I}\mathcal{S}$, respectively.

$(s_c - D) \pmod 2$	$D \pmod 2$	\mathcal{M}	\mathcal{T}	\mathcal{P}	\mathcal{S}	\mathcal{I}	$\sigma_{\mathcal{T}}$	$\sigma_{\mathcal{P}}$	$\sigma_{\mathcal{S}}$	
0	0	Γ_{d+k}	0	0	0	Γ_{d+k}	0	0	0	
	1	Γ_{d+k+1}	0	0	Γ_{d+k}	Γ_{d+k+1}	0	0	-	
$(s_r - D) \pmod 8$	$D \pmod 4$	\mathcal{M}	\mathcal{T}	\mathcal{P}	\mathcal{S}	\mathcal{I}	$\sigma_{\mathcal{T}}$	$\sigma_{\mathcal{P}}$	$\sigma_{\mathcal{S}}$	
0	0	Γ_{d+k}	\mathcal{A}	0	0	Γ_{d+k}	+	0	0	
	1	Γ_{d+k+1}	$\Gamma_{d+k}\mathcal{A}$	\mathcal{A}	Γ_{d+k}	Γ_{d+k+1}	+	-	-	
	2	Γ_{d+k}	0	\mathcal{A}	0	Γ_{d+k}	0	-	0	
	3	Γ_{d+k+1}	\mathcal{A}	$\Gamma_{d+k}\mathcal{A}$	Γ_{d+k}	Γ_{d+k+1}	+	-	-	
1	0	Γ_{d+k+2}	\mathcal{A}	$\Gamma_{d+k}\mathcal{A}$	Γ_{d+k}	Γ_{d+k+2}	+	-	-	
						$i\Gamma_{d+k}\Gamma_{d+k+1}\Gamma_{d+k+2}$	+	+	+	
	1	Γ_{d+k+1}	0	\mathcal{A}	0	Γ_{d+k+1}	0	-	0	
	2	Γ_{d+k+2}	$\Gamma_{d+k}\mathcal{A}$	\mathcal{A}	Γ_{d+k}	Γ_{d+k+2}	+	-	-	
						$i\Gamma_{d+k}\Gamma_{d+k+1}\Gamma_{d+k+2}$	-	-	-	
2	0	Γ_{d+k+2}	0	$\Gamma_{d+k}\mathcal{A}$	0	Γ_{d+k+2}	0	-	0	
						$i\Gamma_{d+k}\Gamma_{d+k+1}\Gamma_{d+k+2}$	0	+	0	
	1	Γ_{d+k+3}	$\Gamma_{d+k+1}\mathcal{A}$	\mathcal{A}	Γ_{d+k+1}	Γ_{d+k+3}	+	-	-	
						$i\Gamma_{d+k}\Gamma_{d+k+1}\Gamma_{d+k+3}$	-	-	+	
						$i\Gamma_{d+k}\Gamma_{d+k+2}\Gamma_{d+k+3}$	-	+	-	
						$i\Gamma_{d+k+1}\Gamma_{d+k+2}\Gamma_{d+k+3}$	-	-	+	
3	0	Γ_{d+k+2}	$\Gamma_{d+k}\mathcal{A}$	0	0	Γ_{d+k+2}	+	0	0	
						$i\Gamma_{d+k}\Gamma_{d+k+1}\Gamma_{d+k+2}$	-	0	0	
	1	Γ_{d+k+3}	\mathcal{A}	$\Gamma_{d+k+1}\mathcal{A}$	Γ_{d+k+1}	Γ_{d+k+3}	+	-	-	
						$i\Gamma_{d+k}\Gamma_{d+k+1}\Gamma_{d+k+3}$	+	+	+	
						$i\Gamma_{d+k}\Gamma_{d+k+2}\Gamma_{d+k+3}$	-	+	-	
						$i\Gamma_{d+k+1}\Gamma_{d+k+2}\Gamma_{d+k+3}$	+	+	+	
4	0	$i\Gamma_{d+k}\Gamma_{d+k+1}\Gamma_{d+k+2}$	\mathcal{A}	0	0	$i\Gamma_{d+k}\Gamma_{d+k+1}\Gamma_{d+k+2}$	+	0	0	
						Γ_{d+k}	+	0	0	
						Γ_{d+k+1}	-	0	0	
							Γ_{d+k+2}	+	0	0
	1	$i\Gamma_{d+k+1}\Gamma_{d+k+2}\Gamma_{d+k+3}$	$\Gamma_{d+k}\mathcal{A}$	\mathcal{A}	Γ_{d+k}	$i\Gamma_{d+k+1}\Gamma_{d+k+2}\Gamma_{d+k+3}$	+	-	-	
						Γ_{d+k+1}	+	-	-	
						Γ_{d+k+2}	-	+	-	
							Γ_{d+k+3}	+	-	-
	2	$i\Gamma_{d+k}\Gamma_{d+k+1}\Gamma_{d+k+2}$	0	\mathcal{A}	0	$i\Gamma_{d+k}\Gamma_{d+k+1}\Gamma_{d+k+2}$	0	-	0	
						Γ_{d+k}	0	-	0	
						Γ_{d+k+1}	0	+	0	
							Γ_{d+k+2}	0	-	0
3	$i\Gamma_{d+k+1}\Gamma_{d+k+2}\Gamma_{d+k+3}$	\mathcal{A}	$\Gamma_{d+k}\mathcal{A}$	Γ_{d+k}	$i\Gamma_{d+k+1}\Gamma_{d+k+2}\Gamma_{d+k+3}$	+	-	-		
					Γ_{d+k+1}	+	-	-		
					Γ_{d+k+2}	-	+	-		
					Γ_{d+k+3}	+	-	-		